

On Regularization via Frame Decompositions with Applications in Tomography

Simon Hubmer*, Ronny Ramlau^{†‡}, Lukas Weissinger[§]

March 23, 2022

Abstract

In this paper, we consider linear ill-posed problems in Hilbert spaces and their regularization via frame decompositions, which are generalizations of the singular-value decomposition. In particular, we prove convergence for a general class of continuous regularization methods and derive convergence rates under both a-priori and a-posteriori parameter choice rules. Furthermore, we apply our derived results to a standard tomography problem based on the Radon transform.

Keywords. Frame Decomposition, Singular-Value Decomposition, Inverse and Ill-Posed Problems, Regularization Theory, Computerized Tomography

1 Introduction

In this paper, we consider linear inverse problems in the standard form

$$Ax = y, \tag{1.1}$$

where $A : X \rightarrow Y$ is a bounded linear operator between real or complex Hilbert spaces X and Y . Additionally, we assume that A is compact, which implies both that solving (1.1) is an ill-posed problem, and that there exists a *singular system* $(\sigma_k, v_k, u_k)_{k=1}^{\infty}$ such that A admits a *singular-value decomposition* (SVD) of the following form (cf. e.g., [10]):

$$Ax = \sum_{k=1}^{\infty} \sigma_k \langle x, v_k \rangle_X u_k. \tag{1.2}$$

Hereby, the *singular values* σ_k and the *singular functions* u_k, v_k are defined as follows:

*Johann Radon Institute Linz, Altenbergerstraße 69, A-4040 Linz, Austria, (simon.hubmer@ricam.oeaw.ac.at), Corresponding author.

[†]Johannes Kepler University Linz, Institute of Industrial Mathematics, Altenbergerstraße 69, A-4040 Linz, Austria, (ronny.ramlau@jku.at)

[‡]Johann Radon Institute Linz, Altenbergerstraße 69, A-4040 Linz, Austria, (ronny.ramlau@ricam.oeaw.ac.at)

[§]Johannes Kepler University Linz, Doctoral Program Computational Mathematics, Altenbergerstraße 69, A-4040 Linz, Austria (lukas.weissinger@dk-compmath.jku.at)

1. The sequence $\{\sigma_k^2\}_{k=1}^\infty$ consists of the non-zero eigenvalues of A^*A written down in decreasing order, taking multiplicity into account and observing $\sigma_k > 0$.
2. The sequence $\{v_k\}_{k=1}^\infty$ is a corresponding complete orthonormal system of eigenfunctions, i.e., it satisfies

$$A^*Av_k = \sigma_k^2v_k. \quad (1.3)$$

Consequently, it spans $\overline{R(A^*)} = N(A)^\perp$.

3. The singular functions u_k are defined by $u_k := (1/\sigma_k)Av_k$. Hence, they satisfy $AA^*u_k = \sigma_k^2u_k$ and form a complete orthonormal system spanning $\overline{R(A)}$.

Note that due to the above definition, the singular functions u_k and v_k satisfy

$$\sigma_k u_k = Av_k, \quad \text{and} \quad \sigma_k v_k = A^*u_k. \quad (1.4)$$

The SVD is an important tool for analysing and solving ill-posed problems. In particular, the *minimum-norm least-squares solution* x^\dagger of (1.1) is characterized by

$$x^\dagger := A^\dagger y := \sum_{k=1}^\infty \frac{\langle y, u_k \rangle_Y}{\sigma_k} v_k, \quad (1.5)$$

which is well-defined if and only if the so-called *Picard condition* holds:

$$\sum_{k=1}^\infty \frac{|\langle y, u_k \rangle_Y|^2}{\sigma_k^2} < \infty. \quad (1.6)$$

Furthermore, given noisy data y^δ , which are typically assumed to satisfy

$$\|y - y^\delta\|_Y \leq \delta, \quad (1.7)$$

where δ denotes the *noise level*, one can define stable approximations x_α^δ of x^\dagger by

$$x_\alpha^\delta := \sum_{k=1}^\infty \sigma_k g_\alpha(\sigma_k^2) \langle y^\delta, u_k \rangle v_k, \quad (1.8)$$

where g_α is a properly selected approximation of $s \mapsto 1/s$. If the *regularization parameter* α is suitably chosen, e.g., by an a-priori or an a-posteriori parameter choice rule [9], then one can prove that $x_\alpha^\delta \rightarrow x^\dagger$ as $\delta \rightarrow 0$. Furthermore, if, e.g., the *source condition*

$$x^\dagger \in R((A^*A)^\mu) \quad (1.9)$$

holds, then one can even prove (order-optimal) convergence rates of the form [10, 20]

$$\|x_\alpha^\delta - x^\dagger\|_X = \mathcal{O}\left(\delta^{\frac{2\mu}{2\mu+1}}\right).$$

Most classic regularization methods can be identified with specific choices of g_α , which are also called *spectral filter functions*. For example, for *Tikhonov regularization*, *Landweber iteration*, or the *truncated singular-value decomposition (TSVD)*, there respectively holds [10, 20]

$$g_\alpha(s) = \begin{cases} (s + \alpha)^{-1}, & \text{Tikhonov,} \\ s^{-1} (1 - (1 - s)^{1/\alpha}), & \text{Landweber,} \\ \begin{cases} 1/s, & s \geq \alpha, \\ 0, & \text{else,} \end{cases} & \text{TSVD.} \end{cases} \quad (1.10)$$

Unfortunately, for many operators no explicit representation of the SVD is known, and even if it is, its numerical computation might be infeasible (see, e.g., [22]). Additionally, generalizing an available SVD of an operator defined between Hilbert spaces over regular domains to irregular domains is often impossible, e.g. in case orthogonality is lost. The situation is somewhat better for finite-dimensional problems, where one can work with the analogously defined SVD of a matrix, but this can also become infeasible when the problem is medium- to large-scale. Hence, even though an important tool in the analysis of ill-posed problems, the SVD often only enjoys limited use in practice.

In order to remedy this situation, several researchers have studied generalizations of the SVD such as the *Wavelet-Vaguelette Decomposition (WVD)* [1, 6, 7, 12, 18, 19] or the *Frame Decomposition (FD)* [8, 13, 15, 16]. The idea is that by weakening some of the requirements of the SVD such as the eigenvalue properties and the resulting orthogonality of the functions u_k and v_k , one may end up with decompositions similar to (1.2) and (1.5) which are easier to derive explicitly for a given operator. For example, the WVD requires an orthonormal wavelet basis $\{\psi_{jk}\}_{j,k \in \mathbb{N}}$ on X and two bi-orthogonal sets (vaguelettes) $\{u_{jk}\}_{j,k \in \mathbb{N}}$, $\{v_{jk}\}_{j,k \in \mathbb{N}}$ on Y , connected by the quasi-singular relations

$$\lambda_{jk} v_{jk} = A \psi_{jk}, \quad \text{and} \quad \lambda_{jk} \psi_{jk} = A^* u_{jk}, \quad \forall j, k \in \mathbb{N}. \quad (1.11)$$

which are reminiscent of (1.4). The resulting decomposition of the operator A is similar to (1.2) and can be used for solving (1.1). For applications of the WVD to the practically relevant problems of computerized and photoacoustic tomography including different aspects of its numerical realization see e.g. [7, 11, 12]. Extensions of the WVD which also have applications to the two- and three- dimensional Radon transform are e.g. given by the biorthogonal curvelet and shearlet decompositions [2, 4].

In contrast to the WVD, the FD does not specifically work with (orthogonal) wavelets and vaguelettes but with general frames in Hilbert spaces; cf. Section 2.1. In particular, the FD requires a frame $\{e_k\}_{k \in \mathbb{N}}$ over X and a frame $\{f_k\}_{k \in \mathbb{N}}$ over Y , connected via

$$\bar{\lambda}_k e_k = A^* f_k, \quad \forall k \in \mathbb{N}, \quad (1.12)$$

where $\bar{\lambda}_k$ denotes the complex conjugate of the coefficient $\lambda_k \in \mathbb{C}$. The above condition is clearly connected to (1.4) and (1.11), and leads to the following decomposition:

$$Ax = \sum_{k=1}^{\infty} \lambda_k \langle x, e_k \rangle_X \tilde{f}_k, \quad \forall x \in X. \quad (1.13)$$

Here the functions $\{\tilde{f}_k\}_{k \in \mathbb{N}}$ denote the dual frame of the frame $\{f_k\}_{k \in \mathbb{N}}$; cf. Section 2.1. Furthermore, for $y \in Y$ one can then analogously to (1.5) consider the operator

$$\mathcal{A}y := \sum_{\substack{k=1 \\ \lambda_k \neq 0}}^{\infty} \frac{1}{\lambda_k} \langle y, f_k \rangle_Y \tilde{e}_k, \quad (1.14)$$

which is well-defined if the following analog of the Picard condition (1.6) holds:

$$\sum_{\substack{k=1 \\ \lambda_k \neq 0}}^{\infty} \frac{|\langle y, f_k \rangle_Y|^2}{|\lambda_k|^2} < \infty. \quad (1.15)$$

The properties of the operator \mathcal{A} and its use for obtaining (approximate) solutions of (1.1) was studied in detail in [16]. In particular, it was investigated in which cases $\mathcal{A}y$ is either a minimum-coefficient or a minimum-norm (least-squares) solution of (1.1). While we refer to [16] for details, we here only want to mention the special case that A satisfies a stability condition of the form

$$c_1 \|x\|_X \leq \|Ax\|_Z \leq c_2 \|x\|_X, \quad \forall x \in X, \quad (1.16)$$

for some constants $c_1, c_2 > 0$ with $Z \subseteq Y$ being a Hilbert space. In this case, for each $y \in R(A)$ the unique solution of (1.1) is precisely given by $\mathcal{A}y$. Furthermore, in this case it is possible to give recipes for finding frames $\{e_k\}_{k \in \mathbb{N}}$ and $\{f_k\}_{k \in \mathbb{N}}$ which satisfy (1.12). For example, starting with a frame $\{f_k\}_{k \in \mathbb{N}}$ which satisfies the condition

$$a_1 \|y\|_Z^2 \leq \sum_{k=1}^{\infty} \alpha_k^2 |\langle y, f_k \rangle_Y|^2 \leq a_2 \|y\|_Z^2, \quad \forall y \in Y, \quad (1.17)$$

for a sequence of coefficients $0 \neq \alpha_k \in \mathbb{R}$ and some constants $a_1, a_2 > 0$, one can define

$$e_k := \alpha_k A^* f_k, \quad \forall k \in \mathbb{N},$$

and it then follows that $\{e_k\}_{k \in \mathbb{N}}$ forms a frame over X satisfying (1.12) with $\bar{\lambda}_k = 1/\alpha_k$ [16]. A typical example for an operator satisfying condition (1.16) is given by the Radon transform [20, 21], and (1.17) can e.g. be satisfied if Y and Z are (suitably connected) Sobolev spaces and $\{f_k\}_{k \in \mathbb{N}}$ is either an exponential or a wavelet frame/basis. Note also that condition (1.16) is satisfied for any continuously invertible operator A with $Z = X$, in which case also (1.17) holds for any frame $\{f_k\}_{k \in \mathbb{N}}$ over Y . Further details on all of these topics can be found in [16], which also includes a generalization of condition (1.12) that can be useful if the Hilbert spaces X and Y have a particular product structure [15, 16, 24].

In this paper, we focus on different aspects of regularization via FDs. In particular, analogously to (1.8) for the SVD we consider stable approximations of $\mathcal{A}y$ of the form

$$z_\alpha^\delta := \sum_{\substack{k=1 \\ \lambda_k \neq 0}}^{\infty} \lambda_k g_\alpha(\lambda_k^2) \langle y^\delta, f_k \rangle_Y \tilde{e}_k,$$

and derive convergence and convergence rate results under a-priori and a-posteriori parameter choice rules similar to those for the SVD [10].

In this context, we want to note that different aspects of regularization via WVDs and specific FDs have already been considered in the literature [8, 12, 13]. For example, a WVD approach to photoacoustic tomography was developed in [12], where regularization with wavelet sparsity constraints is employed via a soft-thresholding approach. This was generalized to sparse regularization for inverse problems using FDs and non-linear soft-thresholding in [13], where also convergence rates were proven under a-priori parameter choice rules. The analysis in [13] is based on the assumption that $\{f_k\}_{k \in \mathbb{N}}$ forms a frame over $\overline{R(A)}$ instead of over Y as in our current setting. The same is also assumed in the preprint [8], in addition to the requirement that $\{e_k\}_{k \in \mathbb{N}}$ forms a frame over $N(A)^\perp = \overline{R(A^*)}$ and that $\lambda_k \in (0, \infty)$ for all $k \in \mathbb{N}$. Note that under these assumptions, for all $y \in D(A^\dagger)$ there holds $A^\dagger y = \mathcal{A}y$. Working within this setting, the authors of [8] prove convergence and convergence rates under a-priori parameter choice rules for continuous regularization methods based on FDs similar to our results.

In contrast to these papers, here we consider the general FD setup introduced above, i.e., we allow arbitrary $\lambda_k \in \mathbb{C}$ and assume that $\{e_k\}_{k \in \mathbb{N}}$ and $\{f_k\}_{k \in \mathbb{N}}$ form frames over X and Y , respectively. This setting is beneficial, since it allows more general and potentially different frame decompositions of a given operator. Furthermore, it is often easier to find a frame over the whole space Y instead of over $\overline{R(A)}$. Note also that (1.12) does not necessarily imply that the frame functions e_k are elements in $N(A)^\perp = \overline{R(A^*)}$, since the coefficients $\lambda_k \in \mathbb{C}$ might be zero as well. This is in fact a crucial difference, since under the assumptions of [8] one has $A^\dagger y = \mathcal{A}y$, which is not necessarily the case in our more general setting (see above). Hence, while [8] considers the stable approximation of $A^\dagger y$ in the presence of noisy data via its representation in terms of frames, here we consider the stable approximation of the (approximate) solution $\mathcal{A}y$. Finally, note that in contrast to [8] we also present convergence rates results for an a-posteriori parameter choice rule adapted from the discrepancy principle, as well as numerical results illustrating our derived theory on the example of a standard tomography problem based on the Radon transform.

The outline of this paper is as follows: In Section 2, after reviewing some necessary material on frames in Hilbert spaces, we consider continuous regularization methods based on frame decompositions and show convergence and convergence rates under standard assumptions, both under a-priori and a-posteriori parameter choice rules. In Section 3, we then apply our results to a standard tomography problem based on the Radon transform, providing numerical examples for specific FDs and comparing the results of different regularization methods. Section 4 then summarizes our results.

2 Regularization via Frame Decompositions

2.1 Background on Frames in Hilbert Spaces

Before deriving our results on regularization via FDs, we first recall some basic facts on frames in Hilbert spaces. This short summary, based on the seminal work [5], is adapted from our previous publications [15, 16]. First, recall the definition of a frame.

Definition 2.1. A sequence $\{e_k\}_{k \in \mathbb{N}}$ in a Hilbert space X is called a frame over X , if and only if there exist *frame bounds* $0 < B_1, B_2 \in \mathbb{R}$ such that for all $x \in X$ there holds

$$B_1 \|x\|_X^2 \leq \sum_{k=1}^{\infty} |\langle x, e_k \rangle_X|^2 \leq B_2 \|x\|_X^2. \quad (2.1)$$

For a given frame $\{e_k\}_{k \in \mathbb{N}}$ one can consider the *frame (analysis) operator* F and its adjoint (*synthesis*) operator F^* , which are given by

$$\begin{aligned} F : X &\rightarrow \ell_2(\mathbb{N}), & x &\mapsto \{\langle x, e_k \rangle_X\}_{k \in \mathbb{N}}, \\ F^* : \ell_2(\mathbb{N}) &\rightarrow X, & \{a_k\}_{k \in \mathbb{N}} &\mapsto \sum_{k=1}^{\infty} a_k e_k. \end{aligned} \quad (2.2)$$

Due to (2.1) there holds

$$\sqrt{B_1} \leq \|F\| = \|F^*\| \leq \sqrt{B_2}. \quad (2.3)$$

Furthermore, one can define the operator $S := F^*F$, i.e.,

$$Sx := \sum_{k=1}^{\infty} \langle x, e_k \rangle_X e_k, \quad (2.4)$$

which is a bounded and continuously invertible linear operator with $B_1 I \leq S \leq B_2 I$ and $B_2^{-1} I \leq S^{-1} \leq B_1^{-1} I$. Hence, it follows that with $\tilde{e}_k := S^{-1} e_k$ there holds

$$B_2^{-1} \|x\|_X^2 \leq \sum_{k=1}^{\infty} |\langle x, \tilde{e}_k \rangle_X|^2 \leq B_1^{-1} \|x\|_X^2, \quad (2.5)$$

for all $x \in X$, and thus the set $\{\tilde{e}_k\}_{k \in \mathbb{N}}$ also forms a frame over X with frame bounds B_2^{-1}, B_1^{-1} which is called the *dual frame* of $\{e_k\}_{k \in \mathbb{N}}$. For the corresponding operators

$$\begin{aligned} \tilde{F} : X &\rightarrow \ell_2(\mathbb{N}), & x &\mapsto \{\langle x, \tilde{e}_k \rangle_X\}_{k \in \mathbb{N}}, \\ \tilde{F}^* : \ell_2(\mathbb{N}) &\rightarrow X, & \{a_k\}_{k \in \mathbb{N}} &\mapsto \sum_{k=1}^{\infty} a_k \tilde{e}_k. \end{aligned} \quad (2.6)$$

it follows analogously to (2.3) that

$$\sqrt{1/B_2} \leq \|\tilde{F}\| = \|\tilde{F}^*\| \leq \sqrt{1/B_1}. \quad (2.7)$$

In particular, for any sequence of coefficients $a = \{a_k\}_{k \in \mathbb{N}}$ there holds

$$\left\| \sum_{k \in \mathbb{N}} a_k \tilde{e}_k \right\|_X = \left\| \tilde{F}^* a \right\|_X \leq \sqrt{1/B_1} \|a\|_{\ell_2(\mathbb{N})}. \quad (2.8)$$

Furthermore, it can be shown that there holds

$$\tilde{F}^* F = F^* \tilde{F} = I,$$

and thus any $x \in X$ can be written in the form

$$x = \sum_{k=1}^{\infty} \langle x, \tilde{e}_k \rangle_X e_k = \sum_{k=1}^{\infty} \langle x, e_k \rangle_X \tilde{e}_k. \quad (2.9)$$

Note that for any frame $\{e_k\}_{k \in \mathbb{N}}$ the following statements are equivalent (see, e.g., [3]):

$$\begin{aligned} N(F^*) = 0 &\Leftrightarrow \{e_k\}_{k \in \mathbb{N}} \text{ is a (Riesz) basis} \\ &\Leftrightarrow \{e_k\}_{k \in \mathbb{N}} \text{ and } \{\tilde{e}_k\}_{k \in \mathbb{N}} \text{ are biorthogonal} \\ &\Leftrightarrow \{e_k\}_{k \in \mathbb{N}} \text{ is exact (i.e. no element can be deleted)}. \end{aligned} \quad (2.10)$$

In general there holds $\{0\} \subset N(F^*) = N(\tilde{F}^*)$, and thus the decomposition of x given in (2.9) is not unique, which is a key difference between frames and bases. However, this decomposition can be understood as the *most economical* one (cf. [5]).

2.2 Continuous Regularization Methods

In this section, we consider general continuous regularization methods based on FDs similar to those based on the SVD [10]. More precisely, for $\alpha > 0$ we consider the functions

$$z_\alpha^\delta = \sum_{\substack{k=1 \\ \lambda_k \neq 0}}^{\infty} \lambda_k g_\alpha(\lambda_k^2) \langle y^\delta, f_k \rangle_Y \tilde{e}_k, \quad (2.11)$$

as approximations of $\mathcal{A}y$ given noisy data y^δ , as well as the functions

$$z_\alpha = \sum_{\substack{k=1 \\ \lambda_k \neq 0}}^{\infty} \lambda_k g_\alpha(\lambda_k^2) \langle y, f_k \rangle_Y \tilde{e}_k, \quad (2.12)$$

in the noise-free case. Here, $g_\alpha : \mathbb{C} \rightarrow \mathbb{C}$ is a suitable approximation of $s \mapsto 1/s$ to be specified below. We will prove convergence as well as convergence rates of the form

$$\|\mathcal{A}y - z_\alpha^\delta\|_Y = \mathcal{O}\left(\delta^{\frac{2\mu}{2\mu+1}}\right)$$

for both a-priori and a-posterior parameter choice rules under standard assumptions. Throughout the analysis, which is based on classical arguments (see e.g. [10]), we use

Assumption 2.1. The operator $A : X \rightarrow Y$ is bounded, linear, and compact between the (complex) Hilbert spaces X and Y . Furthermore, the set $\{e_k\}_{k \in \mathbb{N}}$ forms a frame over X with frame bounds B_1, B_2 , and the set $\{f_k\}_{k \in \mathbb{N}}$ forms a frame over Y with frame bounds C_1, C_2 . Moreover, there exist coefficients $\lambda_k \in \mathbb{C}$ such that (1.12) holds. In addition, let $g_\alpha : \mathbb{C} \rightarrow \mathbb{C}$ be a parameter-dependent family of piecewise continuous, bounded functions defined for all $\alpha > 0$, satisfying

$$\lim_{\alpha \rightarrow 0} g_\alpha(\lambda) = \frac{1}{\lambda}, \quad \forall \lambda \in \mathbb{C}. \quad (2.13)$$

Additionally, assume there exists a constant $C > 0$ independent of α such that

$$|\lambda g_\alpha(\lambda)| \leq C, \quad \forall \lambda \in \mathbb{C}. \quad (2.14)$$

Note that (2.13) and (2.14), as well as the following definitions, which we need for the upcoming analysis, are the same as those used in the classic SVD analysis [10, 20]:

Definition 2.2. For all $\alpha > 0$ we define

$$r_\alpha(\lambda) := 1 - \lambda g_\alpha(\lambda), \quad (2.15)$$

as well as

$$G_\alpha := \sup \{ |g_\alpha(\lambda)| \mid \lambda \in \mathbb{C} \}. \quad (2.16)$$

Furthermore,

$$\gamma := \sup \{ |r_\alpha(\lambda)| \mid \alpha > 0, \lambda \in \mathbb{C} \} \stackrel{(2.14)}{\leq} (C + 1). \quad (2.17)$$

Next, concerning the well-definedness of z_α^δ and z_α we have

Lemma 2.1. *Let Assumption 2.1 hold and let $y, y^\delta \in Y$. Then z_α^δ and z_α as given in (2.11) and (2.12) are well-defined. Furthermore, if additionally the Picard condition (1.15) holds, then $\mathcal{A}y$ given in (1.14) is well-defined.*

Proof. Let $y \in Y$ be arbitrary but fixed. Since the set $\{e_k\}_{k \in \mathbb{N}}$ forms a frame over X with frame bounds B_1, B_2 , it follows from (2.8) that

$$\|z_\alpha\|_Y^2 \leq (1/B_1) \sum_{\substack{k=1 \\ \lambda_k \neq 0}}^{\infty} |\lambda_k g_\alpha(\lambda_k^2) \langle y, f_k \rangle_Y|^2 \stackrel{(2.14)}{\leq} (C/B_1) \|g_\alpha\|_\infty \sum_{\substack{k=1 \\ \lambda_k \neq 0}}^{\infty} |\langle y, f_k \rangle_Y|^2.$$

Furthermore, since $\{f_k\}_{k \in \mathbb{N}}$ forms a frame over Y with bounds C_1, C_2 , it follows that

$$\|z_\alpha\|_Y^2 \leq C_2(C/B_1) \|g_\alpha\|_\infty \|y\|_Y^2.$$

Hence, since we assumed that g_α is bounded it follows that z_α is well-defined. Analogously we can show that z_α^δ is well-defined. Furthermore, similarly to above we have

$$\|\mathcal{A}y\|_Y^2 \leq (1/B_1) \sum_{\substack{k=1 \\ \lambda_k \neq 0}}^{\infty} \left| \frac{\langle y, f_k \rangle_Y}{\lambda_k} \right|^2 \stackrel{(1.15)}{<} \infty.$$

Hence, if (1.15) is satisfied then also $\mathcal{A}y$ is well-defined, which concludes the proof. \square

The following result establishes convergence of z_α to $\mathcal{A}y$ in the noise-free case.

Theorem 2.2. *Let Assumption 2.1 hold and let $y \in Y$ satisfy (1.15). Then for $\mathcal{A}y$ and z_α as defined in (1.14) and (2.12), respectively, there holds*

$$\lim_{\alpha \rightarrow 0} \|\mathcal{A}y - z_\alpha\|_X = 0.$$

Proof. Let $y \in Y$ be arbitrary but fixed and let (1.15) hold. Then due to Lemma 2.1 both $\mathcal{A}y$ and z_α are well-defined. Furthermore, due to (1.14) and (2.12) there holds

$$\mathcal{A}y - z_\alpha = \sum_{\substack{k=1 \\ \lambda_k \neq 0}}^{\infty} (1/\lambda_k - \lambda_k g_\alpha(\lambda_k^2)) \langle y, f_k \rangle_Y \tilde{e}_k = \sum_{\substack{k=1 \\ \lambda_k \neq 0}}^{\infty} \frac{r_\alpha(\lambda_k^2)}{\lambda_k} \langle y, f_k \rangle_Y \tilde{e}_k. \quad (2.18)$$

Since $\{e_k\}_{k \in \mathbb{N}}$ forms a frame with frame bounds B_1, B_2 , it follows from (2.8) that

$$\|\mathcal{A}y - z_\alpha\|_Y^2 \leq \frac{1}{B_1} \sum_{\substack{k=1 \\ \lambda_k \neq 0}}^{\infty} \left| \frac{r_\alpha(\lambda_k^2)}{\lambda_k} \langle y, f_k \rangle_Y \right|^2. \quad (2.19)$$

Since due to (2.14) and the definition of r_α there holds $|r_\alpha(\lambda)| \leq (C+1)$, it follows that

$$\|\mathcal{A}y - z_\alpha\|_Y^2 \leq \frac{(C+1)^2}{B_1} \sum_{\substack{k=1 \\ \lambda_k \neq 0}}^{\infty} \frac{|\langle y, f_k \rangle_Y|^2}{|\lambda_k|^2}.$$

The right-hand side in the above inequality is uniformly bounded independently of α due to (1.15). Hence, we can apply the dominated convergence theorem to obtain

$$\lim_{\alpha \rightarrow 0} \|\mathcal{A}y - z_\alpha\|_X^2 \stackrel{(2.19)}{\leq} \lim_{\alpha \rightarrow 0} \frac{1}{B_1} \sum_{\substack{k=1 \\ \lambda_k \neq 0}}^{\infty} \left| \frac{r_\alpha(\lambda_k^2)}{\lambda_k} \langle y, f_k \rangle_Y \right|^2 \leq \frac{1}{B_1} \sum_{\substack{k=1 \\ \lambda_k \neq 0}}^{\infty} \lim_{\alpha \rightarrow 0} |r_\alpha(\lambda_k^2)|^2 \frac{|\langle y, f_k \rangle_Y|^2}{|\lambda_k|^2}.$$

Since due to (2.13) there holds $\lim_{\alpha \rightarrow 0} r_\alpha(\lambda) = 0$ for all $\lambda \neq 0$, it follows that

$$\lim_{\alpha \rightarrow 0} \|\mathcal{A}y - z_\alpha\|_X = 0,$$

which yields the assertion and thus concludes the proof. \square

Next, we derive an upper bound on the data-propagation error in the following

Theorem 2.3. *Let Assumption 2.1 hold, let $y, y^\delta \in Y$ satisfy (1.7), and let $z_\alpha, z_\alpha^\delta$ be as in (2.12), (2.11), respectively. Then with G_α as defined in (2.16) there holds*

$$\|z_\alpha - z_\alpha^\delta\|_X \leq \delta \sqrt{CC_2/B_1} \sqrt{G_\alpha}.$$

Proof. Let $y, y^\delta \in Y$ satisfying (1.7) be arbitrary but fixed. Then due to Lemma (2.1) both z_α and z_α^δ are well-defined. By their definitions (2.12) and (2.11) it follows that

$$z_\alpha - z_\alpha^\delta = \sum_{\substack{k=1 \\ \lambda_k \neq 0}}^{\infty} \lambda_k g_\alpha(\lambda_k^2) \langle y - y^\delta, f_k \rangle_Y \tilde{e}_k.$$

Since $\{e_k\}_{k \in \mathbb{N}}$ forms a frame with frame bounds B_1, B_2 , it follows from (2.8) that

$$\|z_\alpha - z_\alpha^\delta\|_X^2 \leq \frac{1}{B_1} \sum_{\substack{k=1 \\ \lambda_k \neq 0}}^{\infty} |\lambda_k g_\alpha(\lambda_k^2)|^2 |\langle y - y^\delta, f_k \rangle_Y|^2,$$

and thus together with the definition (2.16) of G_α and (2.14) we get

$$\|z_\alpha - z_\alpha^\delta\|_X^2 \leq \frac{CG_\alpha}{B_1} \sum_{\substack{k=1 \\ \lambda_k \neq 0}}^{\infty} |\langle y - y^\delta, f_k \rangle_Y|^2.$$

Hence, since $\{f_k\}_{k \in \mathbb{N}}$ forms a frame with frame bounds C_1, C_2 , it follows that

$$\|z_\alpha - z_\alpha^\delta\|_X^2 \leq CG_\alpha(C_2/B_1) \|y - y^\delta\|_Y^2 \stackrel{(1.7)}{\leq} CG_\alpha(C_2/B_1) \delta^2,$$

which after taking the square root on both sides yields the assertion. \square

Combining Theorem 2.2 and Theorem 2.3, for the total error we obtain

$$\|\mathcal{A}y - z_\alpha^\delta\|_X \leq \|\mathcal{A}y - z_\alpha\|_X + \delta \sqrt{CC_2/B_1} \sqrt{G_\alpha}, \quad (2.20)$$

where the first term tends to 0 for $\alpha \rightarrow 0$ if y satisfies (1.15), similarly as in the SVD case. Hence, if the regularization parameter $\alpha = \alpha(\delta)$ is chosen such that

$$\alpha(\delta) \rightarrow 0, \quad \text{and} \quad \delta \sqrt{G_{\alpha(\delta)}} \rightarrow 0, \quad \text{as} \quad \delta \rightarrow 0,$$

then we obtain convergence of $z_{\alpha(\delta)}^\delta$ to $\mathcal{A}y$ as the noise level $\delta \rightarrow 0$.

2.3 A-priori Parameter Choice Rules

In this section we derive convergence rates results under a-priori parameter choice rules similar to those for the SVD case (cf. [10]). These typically require source conditions such as the Hölder-type condition (1.9) for some $\mu > 0$. Alternatively, this can be rewritten as

$$\exists w \in X : \quad x^\dagger = (A^*A)^\mu w.$$

Using the SVD (1.3) of the operator A it follows

$$\sigma_k^{-1} \langle y, u_k \rangle_Y = \langle x^\dagger, v_k \rangle_X = \langle (A^*A)^\mu w, v_k \rangle_X = \sigma_k^{2\mu} \langle w, v_k \rangle_X,$$

and thus (1.9) is equivalent to

$$\exists w \in X \forall k \in \mathbb{N} : \quad \langle y, u_k \rangle_Y = \langle (A^*A)^\mu w, v_k \rangle_X = \sigma_k^{2\mu+1} \langle w, v_k \rangle, \quad (2.21)$$

which in turn is equivalent to the decay condition [10, Prop. 3.13]

$$\sum_{k=1}^{\infty} \sigma_k^{-(4\mu+2)} |\langle y, u_k \rangle_Y|^2 < \infty. \quad (2.22)$$

For the upcoming analysis, we use a source condition similar to (2.21), namely

$$\exists w \in X \forall k \in \mathbb{N}, \lambda_k \neq 0 : \quad \langle y, f_k \rangle_Y = \lambda_k^{2\mu+1} \langle w, e_k \rangle_X, \quad (2.23)$$

which analogously to (2.22) implies the decay condition

$$\sum_{\substack{k=1 \\ \lambda_k \neq 0}}^{\infty} |\lambda_k|^{-(4\mu+2)} |\langle y, f_k \rangle_Y|^2 < \infty.$$

We now start our analysis by deriving a convergence rate estimate given exact data.

Theorem 2.4. *Let Assumption 2.1 hold, let $y \in Y$ satisfy (1.15), and let $\mathcal{A}y$ and z_α be as in (1.14) and (2.12), respectively. Moreover, let $\mu > 0$, $\alpha_0 > 0$, and assume that for all $\alpha \in (0, \alpha_0)$ and $\lambda \in \mathbb{C}$ the function r_α defined in (2.15) satisfies*

$$|\lambda|^\mu |r_\alpha(\lambda)| \leq c_\mu \alpha^\mu, \quad (2.24)$$

for some constant $c_\mu > 0$. Then if the source condition (2.23) holds it follows that

$$\|\mathcal{A}y - z_\alpha\|^2 \leq \left\{ \frac{B_2}{B_1} c_\mu^2 \|w\|_X^2 \right\} \alpha^{2\mu}.$$

Proof. Let $y \in Y$ be arbitrary but fixed and let (1.15) hold. Then due to Lemma 2.1 both $\mathcal{A}y$ and z_α are well-defined. Then due to (2.18) there holds

$$\mathcal{A}y - z_\alpha = \sum_{\substack{k=1 \\ \lambda_k \neq 0}}^{\infty} \frac{r_\alpha(\lambda_k^2)}{\lambda_k} \langle y, f_k \rangle_Y \tilde{e}_k,$$

which together with the source condition (2.23) implies

$$\mathcal{A}y - z_\alpha = \sum_{\substack{k=1 \\ \lambda_k \neq 0}}^{\infty} r_\alpha(\lambda_k^2) \lambda_k^{2\mu} \langle w, e_k \rangle_X \tilde{e}_k.$$

Hence, since $\{e_k\}_{k \in \mathbb{N}}$ forms a frame with bounds B_1, B_2 , it follows with (2.8) that

$$\|\mathcal{A}y - z_\alpha\|_X^2 \leq \frac{1}{B_1} \sum_{\substack{k=1 \\ \lambda_k \neq 0}}^{\infty} |r_\alpha(\lambda_k^2) \lambda_k^{2\mu}|^2 |\langle w, e_k \rangle_X|^2.$$

Together with (2.24) this implies

$$\|\mathcal{A}y - z_\alpha\|_X^2 \stackrel{(2.24)}{\leq} \frac{1}{B_1} (c_\mu \alpha^\mu)^2 \sum_{\substack{k=1 \\ \lambda_k \neq 0}}^{\infty} |\langle w, e_k \rangle_X|^2 \stackrel{(2.1)}{\leq} \frac{B_2}{B_1} (c_\mu \alpha^\mu)^2 \|w\|_X^2 ,$$

which yields the assertion. \square

Next, we derive convergence rate estimates also in the case of inexact data.

Theorem 2.5. *Let Assumption 2.1 hold, let $y \in Y$ satisfy (1.15), $y^\delta \in Y$ satisfy (1.7), and let $\mathcal{A}y$ and z_α^δ be as in (1.14) and (2.11), respectively. Moreover, let $\mu > 0$, $\alpha_0 > 0$, and assume that for all $\alpha \in (0, \alpha_0)$ and $\lambda \in \mathbb{C}$ the function r_α defined in (2.15) satisfies (2.24) for some constant $c_\mu > 0$. Furthermore, let (2.23) hold and assume that*

$$G_\alpha = \mathcal{O}(\alpha^{-1}) \quad \text{as } \alpha \rightarrow 0. \quad (2.25)$$

Then with the a-priori parameter choice rule

$$\alpha \sim \delta^{\frac{2}{2\mu+1}}, \quad (2.26)$$

it follows that

$$\|\mathcal{A}y - z_\alpha^\delta\|_X = \mathcal{O}\left(\delta^{\frac{2\mu}{2\mu+1}}\right).$$

Proof. Let $y, y^\delta \in Y$ satisfying (1.7), (1.15) be arbitrary but fixed. Then by Lemma 2.1 it follows that $z_\alpha, z_\alpha^\delta$, and $\mathcal{A}y$ are well-defined. Furthermore, since there holds

$$\|\mathcal{A}y - z_\alpha^\delta\|_Y \leq \|\mathcal{A}y - z_\alpha\|_Y + \|z_\alpha - z_\alpha^\delta\|_Y ,$$

we can apply Theorem 2.3 and Theorem 2.4 to obtain

$$\|\mathcal{A}y - z_\alpha^\delta\|_Y \leq (B_2/B_1)^{1/2} c_\mu \|w\|_X \alpha^\mu + \delta \sqrt{CC_2/B_1} \sqrt{G_\alpha}.$$

Together with (2.25) this implies that

$$\|\mathcal{A}y - z_\alpha^\delta\|_Y = \mathcal{O}\left(\alpha^\mu + \frac{\delta}{\sqrt{\alpha}}\right),$$

which together with the a-priori choice (2.26) yields

$$\|\mathcal{A}y - z_\alpha^\delta\|_Y = \mathcal{O}\left(\delta^{\frac{2\mu}{2\mu+1}}\right),$$

and thus concludes the proof. \square

Remark 2.1. Note that (2.24) could be replaced by the more general condition

$$|\lambda|^\mu |r_\alpha(\lambda)| \leq \omega_\mu(\alpha),$$

for some function $\omega_\mu : (0, \alpha_0) \rightarrow \mathbb{R}$. With this, one can derive similar results as in Theorem 2.4 and Theorem 2.5 also under more general source conditions than (2.23).

2.4 A-posteriori Parameter Choice Rule

In this section we derive convergence rates results under an a-posteriori parameter choice rule similar to the SVD case. More precisely, we consider a variant of the well-known *discrepancy principle*, which defines the regularization parameter $\alpha^{\text{DP}}(\delta, y^\delta)$ via

$$\alpha^{\text{DP}} = \alpha^{\text{DP}}(\delta, y^\delta) := \sup \{ \alpha > 0 \mid \|Ax_\alpha^\delta - y^\delta\|_Y \leq \tau^{\text{DP}} \delta \}, \quad (2.27)$$

where the constant τ^{DP} is chosen such that

$$\tau^{\text{DP}} > \sup \{ |r_\alpha(\lambda)| \mid \alpha > 0, \lambda \in \mathbb{C} \}.$$

Since from the properties of the SVD it follows (after some computation) that

$$\|Ax_\alpha^\delta - y^\delta\|_Y^2 = \sum_{k=1}^{\infty} |r_\alpha(\sigma_k^2) \langle y^\delta, u_k \rangle_Y|^2 + \|(I - Q)y^\delta\|_Y^2,$$

where Q is the orthogonal projector onto $\overline{R(A)}$, it follows that (2.27) is equivalent to

$$\alpha^{\text{DP}}(\delta, y^\delta) := \sup \left\{ \alpha > 0 \mid \sum_{k=1}^{\infty} |r_\alpha(\sigma_k^2) \langle y^\delta, u_k \rangle_Y|^2 + \|(I - Q)y^\delta\|_Y^2 \leq (\tau^{\text{DP}} \delta)^2 \right\}.$$

This motivates the following a-posteriori parameter choice rule for the FD case:

Definition 2.3. Let γ be as in (2.17) and let the parameter $\tau > 0$ be such that

$$\tau > \sqrt{C_2 \gamma}, \quad (2.28)$$

where as before C_2 denotes the upper frame bound of $\{f_k\}_{k \in \mathbb{N}}$. Then we define

$$\alpha(\delta, y^\delta) := \sup \left\{ \alpha > 0 \mid \sum_{\substack{k=1 \\ \lambda_k \neq 0}}^{\infty} |r_\alpha(\lambda_k^2) \langle y^\delta, f_k \rangle_Y|^2 \leq (\tau \delta)^2 \right\}. \quad (2.29)$$

In case that $\alpha(\delta, y^\delta) = +\infty$, $z_{\alpha(\delta, y^\delta)}^\delta$ is understood in the sense of a limit, i.e.,

$$z_\infty^\delta := \lim_{\alpha \rightarrow \infty} z_\alpha^\delta. \quad (2.30)$$

Remark 2.2. While the SVD is generally not known explicitly and thus mostly used as a theoretical tool, we here assume that the FD is known explicitly. Hence, the sum in (2.29) can be computed and thus our a-posteriori rule can also be used in practice.

Concerning the well-definedness of our parameter choice rule, we have the following

Lemma 2.6. *Let Assumption 2.1 hold, let $y, y^\delta \in Y$ satisfy (1.15), (1.7), respectively, and let the function $\alpha \mapsto g_\alpha(\lambda)$ be continuous from the left for all $\lambda \in \mathbb{C}$. Then the set*

$$D := \left\{ \alpha > 0 \mid \sum_{\substack{k=1 \\ \lambda_k \neq 0}}^{\infty} |r_\alpha(\lambda_k^2) \langle y^\delta, f_k \rangle_Y|^2 \leq (\tau \delta)^2 \right\} \quad (2.31)$$

is non-empty, and thus (2.29) yields a well-defined stopping index $\alpha(\delta, y^\delta)$ in $(0, \infty]$. Furthermore, if $\alpha(\delta, y^\delta) < \infty$ then the supremum in (2.29) is attained, and thus

$$\sum_{\substack{k=1 \\ \lambda_k \neq 0}}^{\infty} |r_{\alpha(\delta, y^\delta)}(\lambda_k^2) \langle y^\delta, f_k \rangle_Y|^2 \leq (\tau\delta)^2. \quad (2.32)$$

Moreover, if additionally G_α as defined in (2.16) satisfies

$$\exists \hat{c} \forall \alpha > 0 : \quad G_\alpha \leq \hat{c}/\alpha, \quad (2.33)$$

then it follows that z_∞^δ as defined in (2.30) satisfies $z_\infty^\delta = 0$.

Proof. Note first that due to (2.1) and (2.17), for all $\alpha > 0$ there holds

$$\sum_{\substack{k=1 \\ \lambda_k \neq 0}}^{\infty} |r_\alpha(\lambda_k^2) \langle y^\delta, f_k \rangle_Y|^2 \leq \gamma^2 C_2 \|y^\delta\|_Y^2.$$

Hence, we can apply the dominated convergence theorem to obtain

$$\lim_{\alpha \rightarrow 0} \sum_{\substack{k=1 \\ \lambda_k \neq 0}}^{\infty} |r_\alpha(\lambda_k^2) \langle y^\delta, f_k \rangle_Y|^2 = \sum_{\substack{k=1 \\ \lambda_k \neq 0}}^{\infty} \lim_{\alpha \rightarrow 0} |r_\alpha(\lambda_k^2)|^2 |\langle y^\delta, f_k \rangle_Y|^2 \stackrel{(2.13)}{=} \stackrel{(2.15)}{=} 0.$$

Hence, for each $\varepsilon > 0$ there exists an $\alpha(\varepsilon)$ such that

$$\sum_{\substack{k=1 \\ \lambda_k \neq 0}}^{\infty} |r_{\alpha(\varepsilon)}(\lambda_k^2) \langle y^\delta, f_k \rangle_Y|^2 \leq \varepsilon,$$

and thus D defined in (2.31) is non-empty and consequently $\alpha(\delta, y^\delta)$ is a well-defined element in $(0, \infty]$. Next, note that since we assumed that for all $\lambda \in \mathbb{C}$ the functional $\alpha \mapsto g_\alpha(\lambda)$ is continuous from the left, it follows that the same is also true for the functional

$$\alpha \mapsto \sum_{\substack{k=1 \\ \lambda_k \neq 0}}^{\infty} |r_\alpha(\lambda_k^2) \langle y^\delta, f_k \rangle_Y|^2.$$

Hence, the supremum in (2.29) is attained and thus (2.32) holds whenever $\alpha(\delta, y^\delta) < \infty$. For the limit case $\alpha(\delta, y^\delta) = \infty$ observe that due to (2.8) and (2.16) there holds

$$\|z_\alpha^\delta\|_X^2 \leq \frac{1}{B_1} \sum_{\substack{k=1 \\ \lambda_k \neq 0}}^{\infty} |\lambda_k g_\alpha(\lambda_k^2) \langle y^\delta, f_k \rangle_Y|^2 \leq \frac{CG_\alpha}{B_1} \sum_{\substack{k=1 \\ \lambda_k \neq 0}}^{\infty} |\langle y^\delta, f_k \rangle_Y|^2.$$

Hence, together with (2.1) and (2.33) we obtain

$$\|z_\alpha^\delta\|_X^2 \leq \frac{CG_\alpha}{B_1} \sum_{\substack{k=1 \\ \lambda_k \neq 0}}^{\infty} |\langle y^\delta, f_k \rangle_Y|^2 \leq \frac{C_2 C}{B_1} \frac{\hat{c}}{\alpha} \|y^\delta\|_Y^2,$$

and thus taking the limit we obtain $z_\infty^\delta = \lim_{\alpha \rightarrow \infty} z_\alpha^\delta = 0$, which concludes the proof. \square

We are now able to derive convergence rate estimates in the presence of noisy data.

Theorem 2.7. *Let Assumption 2.1 hold, let $y \in Y$ satisfy (1.15), $y^\delta \in Y$ satisfy (1.7), and let $\mathcal{A}y$ and z_α^δ be as in (1.14) and (2.11), respectively. Moreover, let $\mu > 0$, $\alpha_0 > 0$, and assume that for all $\alpha \in (0, \alpha_0)$ and $\lambda \in \mathbb{C}$ the function r_α defined in (2.15) satisfies*

$$|\lambda|^{\mu+1/2} |r_\alpha(\lambda)| \leq c_{\mu+1/2} \alpha^{\mu+1/2}, \quad (2.34)$$

for some constant $c_{\mu+1/2} > 0$. Furthermore, let (2.33) and the source condition (2.23) hold, and let the function $\alpha \mapsto g_\alpha(\lambda)$ be continuous from the left for all $\lambda \in \mathbb{C}$. Then for $\alpha = \alpha(\delta, y^\delta)$ chosen via the a-posteriori stopping rule (2.28), (2.29), it follows that

$$\|\mathcal{A}y - z_\alpha^\delta\|_X = \mathcal{O}\left(\delta^{\frac{2\mu}{2\mu+1}}\right).$$

Proof. First, assume that there are sequences $\delta_n \rightarrow 0$ and $y^{\delta_n} \in Y$ satisfying

$$\|y - y^{\delta_n}\|_Y \leq \delta_n,$$

such that for all n there holds $\alpha_n := \alpha(\delta_n, y^{\delta_n}) = \infty$. Then due to (2.29) there holds

$$\sum_{\substack{k=1 \\ \lambda_k \neq 0}}^{\infty} |r_\alpha(\lambda_k^2) \langle y^{\delta_n}, f_k \rangle_Y|^2 \leq (\tau \delta_n)^2,$$

for all $\alpha > 0$. Hence, together with (2.1) and the definition (2.17) of γ we obtain

$$\begin{aligned} \sum_{\substack{k=1 \\ \lambda_k \neq 0}}^{\infty} |r_\alpha(\lambda_k^2) \langle y, f_k \rangle_Y|^2 &\leq 2 \sum_{\substack{k=1 \\ \lambda_k \neq 0}}^{\infty} |r_\alpha(\lambda_k^2) \langle y - y^{\delta_n}, f_k \rangle_Y|^2 + 2 \sum_{\substack{k=1 \\ \lambda_k \neq 0}}^{\infty} |r_\alpha(\lambda_k^2) \langle y^{\delta_n}, f_k \rangle_Y|^2 \\ &\leq 2\gamma^2 C_2 \|y - y^{\delta_n}\|_Y^2 + 2(\tau \delta_n)^2 \leq 2(\gamma^2 C_2 + \tau^2) \delta_n^2. \end{aligned} \quad (2.35)$$

Letting $n \rightarrow \infty$ in the above inequality we thus obtain that for all $\alpha > 0$ there holds

$$\sum_{\substack{k=1 \\ \lambda_k \neq 0}}^{\infty} |r_\alpha(\lambda_k^2) \langle y, f_k \rangle_Y|^2 = 0.$$

Hence, using the dominated convergence theorem we obtain

$$0 = \lim_{\alpha \rightarrow \infty} \sum_{\substack{k=1 \\ \lambda_k \neq 0}}^{\infty} |r_\alpha(\lambda_k^2) \langle y, f_k \rangle_Y|^2 = \sum_{\substack{k=1 \\ \lambda_k \neq 0}}^{\infty} \lim_{\alpha \rightarrow \infty} |r_\alpha(\lambda_k^2)|^2 |\langle y, f_k \rangle_Y|^2.$$

Now since from the definition (2.16) of G_α and (2.33) there follows

$$|r_\alpha(\lambda_k^2)| = |1 - \lambda_k^2 g_\alpha(\lambda_k^2)| \geq 1 - |\lambda_k^2 g_\alpha(\lambda_k^2)| \stackrel{(2.16)}{\geq} 1 - |\lambda_k^2| G_\alpha \stackrel{(2.33)}{\geq} 1 - |\lambda_k^2| \hat{c}/\alpha,$$

we obtain that $\lim_{\alpha \rightarrow \infty} |r_\alpha(\lambda_k^2)| \geq 1$ and thus we find that

$$0 = \sum_{\substack{k=1 \\ \lambda_k \neq 0}}^{\infty} \lim_{\alpha \rightarrow \infty} |r_\alpha(\lambda_k^2)|^2 |\langle y, f_k \rangle_Y|^2 \geq \sum_{\substack{k=1 \\ \lambda_k \neq 0}}^{\infty} |\langle y, f_k \rangle_Y|^2.$$

Since this implies $\langle y, f_k \rangle_Y = 0$ for all $\lambda_k \neq 0$, it follows from the definition of $\mathcal{A}y$ that

$$\mathcal{A}y = 0 = z_{\alpha_n}^{\delta_n}.$$

Hence, for the remainder of this proof we can assume that $\alpha(\delta, y^\delta) < \infty$ for all y^δ satisfying (1.7) with δ sufficiently small. Next, note that in (2.19) we have shown that

$$\|\mathcal{A}y - z_\alpha\|_Y^2 \leq \frac{1}{B_1} \sum_{\substack{k=1 \\ \lambda_k \neq 0}}^{\infty} \left| \frac{r_\alpha(\lambda_k^2)}{\lambda_k} \langle y, f_k \rangle_Y \right|^2.$$

Since by the Hölder inequality with $p = 2\mu + 1$ and $q = (2\mu + 1)/(2\mu)$ there follows

$$\begin{aligned} \sum_{\substack{k=1 \\ \lambda_k \neq 0}}^{\infty} |r_\alpha(\lambda_k^2) \lambda_k^{-1} \langle y, f_k \rangle_Y|^2 &= \sum_{\substack{k=1 \\ \lambda_k \neq 0}}^{\infty} |r_\alpha(\lambda_k^2) \lambda_k^{-(2\mu+1)} \langle y, f_k \rangle_Y|^{\frac{2}{2\mu+1}} |r_\alpha(\lambda_k^2) \langle y, f_k \rangle_Y|^{\frac{4\mu}{2\mu+1}} \\ &\leq \left(\sum_{\substack{k=1 \\ \lambda_k \neq 0}}^{\infty} |r_\alpha(\lambda_k^2) \lambda_k^{-(2\mu+1)} \langle y, f_k \rangle_Y|^2 \right)^{\frac{1}{2\mu+1}} \left(\sum_{\substack{k=1 \\ \lambda_k \neq 0}}^{\infty} |r_\alpha(\lambda_k^2) \langle y, f_k \rangle_Y|^2 \right)^{\frac{2\mu}{2\mu+1}}, \end{aligned}$$

we thus obtain that

$$\|\mathcal{A}y - z_\alpha\|_Y^2 \leq \frac{1}{B_1} \left(\sum_{\substack{k=1 \\ \lambda_k \neq 0}}^{\infty} |r_\alpha(\lambda_k^2) \lambda_k^{-(2\mu+1)} \langle y, f_k \rangle_Y|^2 \right)^{\frac{1}{2\mu+1}} \left(\sum_{\substack{k=1 \\ \lambda_k \neq 0}}^{\infty} |r_\alpha(\lambda_k^2) \langle y, f_k \rangle_Y|^2 \right)^{\frac{2\mu}{2\mu+1}}. \quad (2.36)$$

We now consider each of these sums separately, where we have already shown in (2.35) that the second sum in (2.36) can be estimated by

$$\sum_{\substack{k=1 \\ \lambda_k \neq 0}}^{\infty} |r_\alpha(\lambda_k^2) \langle y, f_k \rangle_Y|^2 \leq 2(\gamma^2 C_2 + \tau^2) \delta^2.$$

Concerning the first sum in (2.36), note that due to the source condition (2.23),

$$\sum_{\substack{k=1 \\ \lambda_k \neq 0}}^{\infty} |r_\alpha(\lambda_k^2) \lambda_k^{-(2\mu+1)} \langle y, f_k \rangle_Y|^2 = \sum_{\substack{k=1 \\ \lambda_k \neq 0}}^{\infty} |r_\alpha(\lambda_k^2) \langle w, e_k \rangle_X|^2.$$

Together with the definition of γ and since $\{e_k\}_{k \in \mathbb{N}}$ forms a frame, we obtain

$$\sum_{\substack{k=1 \\ \lambda_k \neq 0}}^{\infty} \left| r_{\alpha}(\lambda_k^2) \lambda_k^{-(2\mu+1)} \langle y, f_k \rangle_Y \right|^2 = \sum_{\substack{k=1 \\ \lambda_k \neq 0}}^{\infty} \left| r_{\alpha}(\lambda_k^2) \langle w, e_k \rangle_X \right|^2 \leq B_2 \gamma^2 \|w\|_X^2. \quad (2.37)$$

Hence, inserting (2.35) and (2.37) into (2.36) we obtain

$$\|\mathcal{A}y - z_{\alpha}\|_Y^2 \leq \frac{1}{B_1} (B_2 \gamma^2 \|w\|_X^2)^{\frac{1}{2\mu+1}} (2(C_2 \gamma^2 + \tau^2) \delta^2)^{\frac{2\mu}{2\mu+1}},$$

which simplifies to

$$\|\mathcal{A}y - z_{\alpha}\|_Y \leq \left(\frac{1}{B_1} (B_2 \gamma^2 \|w\|_X^2)^{\frac{1}{2\mu+1}} (2(C_2 \gamma^2 + \tau^2))^{\frac{2\mu}{2\mu+1}} \right)^{1/2} \delta^{\frac{2\mu}{2\mu+1}}, \quad (2.38)$$

and thus provides an (optimal) convergence rate given exact data. Next, note that due to the reverse triangle inequality there holds

$$\begin{aligned} \left(\sum_{\substack{k=1 \\ \lambda_k \neq 0}}^{\infty} \left| r_{2\alpha}(\lambda_k^2) \langle y - y^{\delta}, f_k \rangle_Y \right|^2 \right)^{1/2} &\geq \left(\sum_{\substack{k=1 \\ \lambda_k \neq 0}}^{\infty} \left| r_{2\alpha}(\lambda_k^2) \langle y^{\delta}, f_k \rangle_Y \right|^2 \right)^{1/2} \\ &\quad - \left(\sum_{\substack{k=1 \\ \lambda_k \neq 0}}^{\infty} \left| r_{2\alpha}(\lambda_k^2) \langle y, f_k \rangle_Y \right|^2 \right)^{1/2}. \end{aligned} \quad (2.39)$$

By the definition (2.29) of our a-posteriori parameter choice rule we obtain

$$\sum_{\substack{k=1 \\ \lambda_k \neq 0}}^{\infty} \left| r_{2\alpha}(\lambda_k^2) \langle y^{\delta}, f_k \rangle_Y \right|^2 > (\tau \delta)^2.$$

Thus, rearranging (2.39), together with the definition of γ , (1.7), and (2.3) we obtain

$$\begin{aligned} \left(\sum_{\substack{k=1 \\ \lambda_k \neq 0}}^{\infty} \left| r_{2\alpha}(\lambda_k^2) \langle y, f_k \rangle_Y \right|^2 \right)^{1/2} &\geq (\tau \delta) - \gamma \left(\sum_{\substack{k=1 \\ \lambda_k \neq 0}}^{\infty} \left| \langle y - y^{\delta}, f_k \rangle_Y \right|^2 \right)^{1/2} \\ &\geq (\tau \delta) - \gamma \sqrt{C_2} \|y - y^{\delta}\|_Y \geq (\tau - \gamma \sqrt{C_2}) \delta. \end{aligned}$$

Now since due to (2.28) there holds

$$c := \tau - \gamma \sqrt{C_2} > 0,$$

it follows that

$$(c\delta)^2 \leq \sum_{\substack{k=1 \\ \lambda_k \neq 0}}^{\infty} |r_{2\alpha}(\lambda_k^2) \langle y, f_k \rangle_Y|^2 = \sum_{\substack{k=1 \\ \lambda_k \neq 0}}^{\infty} |r_{2\alpha}(\lambda_k^2) \lambda_k^{2\mu+1}|^2 \left| \lambda_k^{-(2\mu+1)} \langle y, f_k \rangle_Y \right|^2.$$

Since due to (2.34) and the definition of γ there holds

$$\left| r_{2\alpha}(\lambda_k^2) \lambda_k^{2\mu+1} \right|^2 \leq (c_{\mu+1/2} (2\alpha)^{\mu+1/2})^2 = c_{\mu+1/2}^2 (2\alpha)^{2\mu+1},$$

it follows together with the source condition (2.23) that

$$(c\delta)^2 \leq c_{\mu+1/2}^2 (2\alpha)^{2\mu+1} \sum_{\substack{k=1 \\ \lambda_k \neq 0}}^{\infty} \left| \lambda_k^{-(2\mu+1)} \langle y, f_k \rangle_Y \right|^2 = c_{\mu+1/2}^2 (2\alpha)^{2\mu+1} \sum_{\substack{k=1 \\ \lambda_k \neq 0}}^{\infty} |\langle w, e_k \rangle_X|^2.$$

Hence, together with (2.1) we obtain

$$(c\delta)^2 \leq c_{\mu+1/2}^2 (2\alpha)^{2\mu+1} B_2 \|w\|_X^2,$$

and thus we find that

$$\alpha^{-1} \leq 2 \left(c_{\mu+1/2} B_2^{1/2} \|w\|_X / c \right)^{\frac{2}{2\mu+1}} \delta^{-\frac{2}{2\mu+1}}. \quad (2.40)$$

Now, note that due to (2.20) and (2.33) there holds

$$\|\mathcal{A}y - z_\alpha^\delta\|_Y \stackrel{(2.20)}{\leq} \|\mathcal{A}y - z_\alpha\|_X + \delta \sqrt{CG_\alpha C_2 / B_1} \stackrel{(2.33)}{\leq} \|\mathcal{A}y - z_\alpha\|_X + \frac{\delta}{\sqrt{\alpha}} \sqrt{\hat{c} C C_2 / B_1}. \quad (2.41)$$

Inserting (2.38) and (2.40) into this inequality yields

$$\begin{aligned} \|\mathcal{A}y - z_\alpha^\delta\|_Y &\leq \left(\frac{1}{B_1} (B_2 \gamma^2 \|w\|_X^2)^{\frac{1}{2\mu+1}} (2(C_2 \gamma^2 + \tau^2))^{\frac{2\mu}{2\mu+1}} \right)^{1/2} \delta^{\frac{2\mu}{2\mu+1}} \\ &\quad + \left(\sqrt{2} \left(c_{\mu+1/2} B_2^{1/2} \|w\|_X / c \right)^{\frac{1}{2\mu+1}} \sqrt{\hat{c} C C_2 / B_1} \right) \delta \delta^{-\frac{1}{2\mu+1}}, \end{aligned}$$

which now yields the assertion. \square

3 Application to the Radon Transform

In this section, we illustrate our theoretical results on continuous regularization via FDs by applying them to a standard tomography problem based on the *Radon transform* [20, 21], which in 2D is given by

$$(Ax)(s, \varphi) := \int_{\mathbb{R}} x(s\omega(\varphi) + t\omega(\varphi)^\perp) dt, \quad (3.1)$$

where $\omega(\varphi) = (\cos(\varphi), \sin(\varphi))^T$ for $\varphi \in [0, 2\pi)$ and $s \in \mathbb{R}$. After recalling some recently derived FDs of the Radon transform on which we base the numerical illustration of our theoretical results derived above, we consider the details of the implementation of these decompositions and provide a number of numerical examples. For comparison, we also present numerical results based on the SVD of the Radon transform; cf. [20, 21].

3.1 Frame Decompositions of the Radon Transform

A number of different decompositions of the Radon transform fitting into the category of frame decompositions have been studied in the past. These include e.g. the WVD [7] or the the biorthogonal curvelet/shearlet decompositions [2, 4], for which also efficient implementations are available. For the numerical examples presented in this paper, which mainly serve to illustrate the theoretical results derived above, we focus on a class of FDs recently introduced in [16]. These are based on a general strategy for deriving FDs for arbitrary bounded linear operators in Hilbert spaces satisfying a stability condition of the form (1.16). In contrast to the classic SVD, available for the setting

$$A : L_2(\Omega_D) \rightarrow L_2(\Omega_S, w^{-1}), \quad w(s) = \sqrt{1 - s^2},$$

where $\Omega_D := \{x \in \mathbb{R}^2 \mid |x| \leq 1\}$ and $\Omega_S := \mathbb{R} \times [0, 2\pi)$, these FDs of the Radon transform are also available for the very general settings

$$A : H_0^\beta(\Omega_D) \rightarrow L_2(\Omega_S), \quad \text{and} \quad A : H_0^\beta(\Omega_D) \rightarrow L_2(\Omega'_S), \quad (3.2)$$

where $\Omega'_S := [-1, 1] \times [0, 2\pi)$. While we refer to [16] for the most general version of these FDs, here we focus only on two special cases based on wavelets and exponentials.

Theorem 3.1. [16, Thm. 5.2] *Let $0 \leq \beta \in \mathbb{R}$ and let $A : H_0^\beta(\Omega_D) \rightarrow L_2(\Omega_S)$ be the Radon transform as defined in (3.1). Furthermore, let $\{\psi_{j,k}\}_{j,k \in \mathbb{Z}}$ be an orthonormal wavelet basis of $L_2(\mathbb{R})$, let $\{w_l\}_{l \in \mathbb{N}}$ be an orthonormal basis of $L_2(0, 2\pi)$, and define*

$$f_{j,k,l}(s, \varphi) := \psi_{j,k}(s)w_l(\varphi), \quad \text{and} \quad e_{j,k,l} := (1 + 2^{-2j(\beta+1/2)})^{1/2} A^* f_{j,k,l}. \quad (3.3)$$

Then the set $\{e_{j,k,l}\}_{j,k \in \mathbb{Z}, l \in \mathbb{N}}$ forms a frame over $H_0^\beta(\Omega_D)$ and

$$Ax = \sum_{j,k \in \mathbb{Z}} \sum_{l=1}^{\infty} (1 + 2^{-2j(\beta+1/2)})^{-1/2} \langle x, e_{j,k,l} \rangle_{H_0^\beta(\Omega_D)} \tilde{f}_{j,k,l} = \sum_{j,k \in \mathbb{Z}} \sum_{l=1}^{\infty} \langle x, A^* f_{j,k,l} \rangle \tilde{f}_{j,k,l}.$$

Furthermore, for any $y \in R(A)$ the unique solution of $Ax = y$ is given by

$$Ax = \sum_{j,k \in \mathbb{Z}} \sum_{l=1}^{\infty} (1 + 2^{-2j(\beta+1/2)})^{1/2} \langle y, f_{j,k,l} \rangle_{L_2(\Omega_S)} \tilde{e}_{j,k,l}. \quad (3.4)$$

A possible choice for the orthonormal basis $\{w_l\}_{l \in \mathbb{N}}$ in the above theorem is e.g.,

$$w_l(\varphi) := (1/\sqrt{2\pi}) \exp(il\varphi),$$

which was also used throughout the numerical experiments presented below.

Theorem 3.2. [16, Remark 5.2] *Let $0 \leq \beta \in \mathbb{R}$ and let $A : H_0^\beta(\Omega_D) \rightarrow L_2(\Omega'_S)$ be the Radon transform as defined in (3.1). Furthermore, let*

$$w_{j,k}(s, \varphi) := \frac{1}{2\sqrt{\pi}} \exp(ij\pi s) \exp(ik\varphi), \quad \text{and} \quad v_{j,k} := (1 + |j|^2)^{(\beta+1/2)/2} A^* w_{j,k}. \quad (3.5)$$

Then the set $\{v_{j,k}\}_{j,k \in \mathbb{Z}}$ forms a frame over $H_0^\beta(\Omega_D)$ and

$$Ax = \sum_{j,k \in \mathbb{Z}} (1 + |j|^2)^{-(\beta+1/2)/2} \langle x, v_{j,k} \rangle_{H_0^\beta(\Omega_D)} \tilde{w}_{j,k} = \sum_{j,k \in \mathbb{Z}} \langle x, A^* w_{j,k} \rangle \tilde{w}_{j,k}.$$

Furthermore, for any $y \in R(A)$ the unique solution of $Ax = y$ is given by

$$\mathcal{A}y = \sum_{j,k \in \mathbb{Z}} (1 + |j|^2)^{(\beta+1/2)/2} \langle y, w_{j,k} \rangle_{L_2(\Omega'_S)} \tilde{v}_{j,k}. \quad (3.6)$$

Note that the FDs and the corresponding formulas for computing $\mathcal{A}y$ given in Theorem 3.1 and 3.2 can be efficiently implemented by approximating the involved inner products via fast Fourier and wavelet transforms. While this can entail a loss of accuracy compared to higher order integration methods, the increased efficiency is beneficial for applications with real-time requirements such as atmospheric tomography [16].

3.2 Implementation and Computational Aspects

In this section, we consider the implementation of the FDs of the Radon transform presented in Section 3.1, focusing on the relevant special case $\beta = 0$ in (3.2), i.e.,

$$A : L_2(\Omega_D) \rightarrow L_2(\Omega_S), \quad \text{and} \quad A : L_2(\Omega_D) \rightarrow L_2(\Omega'_S).$$

The key difference in implementation between the FDs given in Theorem 3.1 and Theorem 3.2 lies in the different sets of frame functions and their corresponding properties. Note that if the dual frame functions $\tilde{e}_{j,k,l}$ or $\tilde{v}_{j,k}$ are pre-computed and stored, then for each right-hand side y the computation of $\mathcal{A}y$ amounts only to the computation of either the inner products $\langle y, f_{j,k,l} \rangle_{L_2(\Omega_S)}$ or $\langle y, w_{j,k} \rangle_{L_2(\Omega'_S)}$, and a corresponding summation according to (3.4) or (3.6), respectively. As mentioned above, these inner products can be efficiently implemented using fast Fourier and wavelet transforms.

3.2.1 Problem Discretization and Computational Environment

For the discretization of the problem we have used the AIR Tools II toolbox [14], which is based on a piecewise constant discretization of both the definition and the image space of A . More precisely, a density function $x \in L_2(\Omega_D)$ is approximated by a piecewise constant function with values given on a uniform $N \times N$ pixel grid. Similarly, sinogram data y are also considered as piecewise constant functions on a uniform $p \times N_\theta$ pixel grid, where p denotes the number of equidistant, parallel lines on $[-1, 1]$, and N_θ denotes the number of different angles θ_n . Hence, the discretized problem can be written as

$$\mathbf{A}\mathbf{x} = \mathbf{y}, \quad \mathbf{x} \in \mathbb{R}^{N^2}, \mathbf{y} \in \mathbb{R}^{pN_\theta}, \mathbf{A} \in \mathbb{R}^{N^2 \times pN_\theta}.$$

For all tests presented below, we have used the choice $N = p = 60$, and $N_\theta = 180$, with uniformly spaced angles $\theta_n = n\pi/180$ for $n = 0, \dots, 179$, which due to $Ax(s, \varphi) = Ax(-s, \varphi + \pi)$ amounts to a full-angle tomography problem. The infinite sums in

formulas (3.4) and (3.6) for computing $\mathcal{A}y$ have been replaced by finite sums as detailed below, and the involved integrals have been approximated using the trapezoidal rule. All computations have been performed using Matlab 2019b on a desktop computer running on Windows 10 with a 4 core processor (Intel Core i5-6500 CPU@3.20GHz) and 16GB RAM, except the computation of the dual frames, which is discussed in detail below, and which was performed on the high performance computing cluster Radon1 [17].

3.2.2 Computation of the Dual Frame Functions

Next, we consider the computation of the dual frame functions \tilde{e}_k . While it is generally not possible to give explicit expressions, one can use the recursive approximation [5]

$$\tilde{e}_k \approx \tilde{e}_k^M = \frac{2}{B_1 + B_2} e_k + \left(I - \frac{2}{B_1 + B_2} S \right) \tilde{e}_k^{M-1}, \quad (3.7)$$

where B_1, B_2 denote the frame bound of $\{e_k\}_{k \in \mathbb{N}}$ and S is as in (2.4). The approximation error can be estimated by [5]:

$$\left\| x - \sum_{k=1}^{\infty} \langle x, e_k \rangle \tilde{e}_k^M \right\|_X \leq \left(\frac{B_2 - B_1}{B_2 + B_1} \right)^{M+1} \|x\|_X. \quad (3.8)$$

Hence, if the frame bounds B_1 and B_2 are close to each other only few iterations are necessary for obtaining an accurate approximation. Unfortunately, for the frames $\{e_{j,k,l}\}_{j,k \in \mathbb{Z}, l \in \mathbb{N}}$ and $\{v_{j,k}\}_{j,k \in \mathbb{Z}}$ in Theorem 3.1 and Theorem 3.2, respectively, the frame bounds depend on constants of a norm-equality estimate like (1.17) which are not known exactly. Hence, for computing an approximation of the dual frame functions via (3.7) a value for $B_1 + B_2$ has to be chosen empirically. On the one hand, one has to choose this value large enough such that the recursion converges, while on the other hand a too large value results in a very slow convergence. For our numerical experiments, we found a value of $B_1 + B_2 = 500$ to lead to satisfactory results within $M = 50$ iterations.

Alternatively, one can compute the dual frame functions \tilde{e}_k directly via their definition $\tilde{e}_k = S^{-1}e_k$. Discretizing as above, one has to solve the system of equations

$$\mathbf{S} \tilde{\mathbf{e}}_k = \mathbf{e}_k, \quad \tilde{\mathbf{e}}_k \in \mathbb{R}^{N^2}, \quad \mathbf{e}_k \in \mathbb{R}^{N^2}, \quad \mathbf{S} \in \mathbb{R}^{N^2 \times N^2},$$

where $\tilde{\mathbf{e}}_k$ and \mathbf{e}_k are piecewise constant discretizations of \tilde{e}_k and e_k , respectively, and

$$\mathbf{S}_{ij} = \left(\sum_{k=1}^{pN_\theta} \langle \phi_i, e_k \rangle \mathbf{e}_k \right)_j,$$

where $\{\phi_i\}_{i \in N^2}$ denotes the piecewise constant pixel basis on Ω_D used for discretization.

Using an LU-decomposition for the matrix \mathbf{S} , the equation $\mathbf{S} \tilde{\mathbf{e}}_k = \mathbf{e}_k$ can be solved efficiently for all k . However, our matrices \mathbf{S} are ill-conditioned, with condition-numbers

$$\kappa_{wav} = \frac{\lambda_{max}}{\lambda_{min}} \approx 7.7 \cdot 10^5, \quad \text{and} \quad \kappa_{exp} = \frac{\lambda_{max}}{\lambda_{min}} \approx 1.5 \cdot 10^5,$$

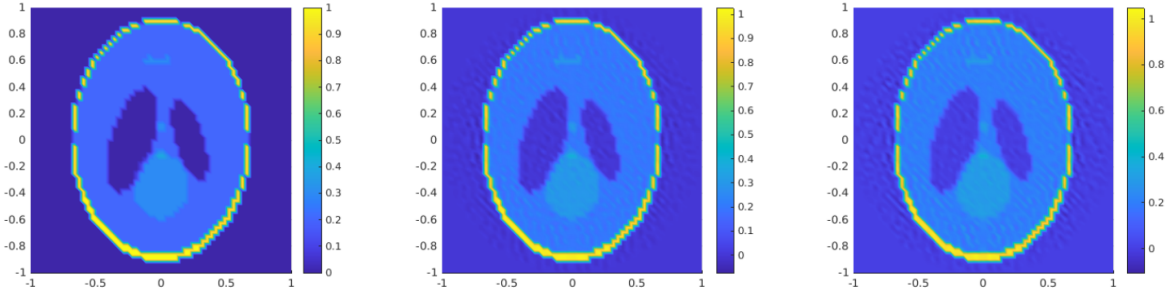


Figure 3.1: Shepp-Logan phantom (left) and its expansion (2.9) in terms of the frame $\{v_{j,k}\}_{j,k \in \mathbb{Z}}$ with the functions $v_{j,k}$ as defined in (3.5) using the explicitly (middle) and the recursively (right) computed dual frames. Note that these computations are based on a coarser discretization with $N_\theta = 90$ instead of $N_\theta = 180$ as explained in the text.

where λ_{max} and λ_{min} denote the maximal and minimal singular value of \mathbf{S} , respectively. Hence, to obtain stable approximations of $\tilde{\mathbf{e}}_k$ we used Tikhonov regularization, i.e.,

$$\tilde{\mathbf{e}}_k \approx (\mathbf{S}^T \mathbf{S} + \alpha I)^{-1} \mathbf{e}_k. \quad (3.9)$$

We found optimal results for $\alpha = 0.01$ for the wavelet-based FD and $\alpha = 2$ for the exponential-based FD. For these particular choices of α , this explicit approach outperformed the recursive approximation. The computed dual frame functions were verified by implementing the reconstruction formula (2.9), an example of which is shown in Figure 3.1. Note that for obtaining these results, a coarser discretization of $N_\theta = 90$ had to be used in the numerical computation of the frame functions $v_{j,k}$ defined via (3.5), since the computation of the recursively approximated dual frames $\tilde{v}_{j,k}$ already takes about 8 hours in this setup, while the full setup with $N_\theta = 180$ angles is computationally infeasible. The reconstructions shown in Figure 3.1 have a relative error of 6.98% in the case of explicitly computed dual frames, and an error of 9.07% in the case of recursively approximated dual frames. Thus, not only is the explicit computation approach faster than the recursive approach, but it also outperforms it in terms of reconstruction quality. Hence, all numerical results presented below are based on the explicitly computed dual frame functions using the full setup with $N_\theta = 180$ angles.

3.2.3 Implementation of the Wavelet-based Frame Decomposition

We now consider the setup from Theorem 3.1. In particular, for $\{\psi_{j,k}\}_{j,k \in \mathbb{Z}}$ we consider inhomogeneous orthonormal wavelet bases of the form $\{\psi_{j_{max},k}^1\}_{k \in \mathbb{Z}} \cap \{\psi_{j,k}^2\}_{j \leq j_{max}, k \in \mathbb{Z}}$. These are defined via $\psi_{j,k}^1(s) = 2^{-j/2} \psi^1(2^{-j}s - k)$ and $\psi_{j,k}^2(s) = 2^{-j/2} \psi^2(2^{-j}s - k)$ based on suitable scaling- and wavelet function ψ^1 and ψ^2 , respectively (cf. [5] for details). A typical example of such wavelet bases are the different Daubechies wavelets [5], for which the corresponding scaling- and wavelet functions are available in Matlab. Using

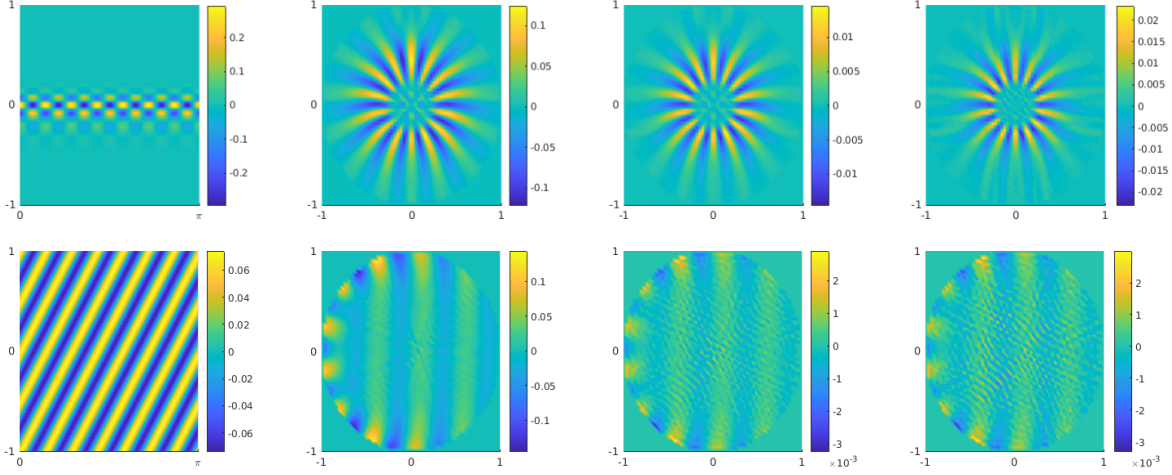


Figure 3.2: Example frame functions based on wavelets (top, $j = 2$, $k = 4$, $l = 7$) and exponential functions (bottom, $j = 4$, $k = 7$). From left to right: f_k , e_k , \tilde{e}_k^M computed with the recursive formula (3.7) and \tilde{e}_k computed explicitly via (3.9).

such an inhomogeneous wavelet basis, any $x \in L_2(\mathbb{R})$ can be written in the form [5]:

$$x = \sum_{k \in \mathbb{Z}} \langle x, \psi_{j_{max}, k}^1 \rangle_{L_2(\mathbb{R})} \psi_{j_{max}, k}^1 + \sum_{j=-\infty}^{j_{max}} \sum_{k \in \mathbb{Z}} \langle x, \psi_{j, k}^2 \rangle_{L_2(\mathbb{R})} \psi_{j, k}^2.$$

In our implementation, we used the ‘db4’ Daubechies-wavelet basis [5], characterized by having 4 vanishing moments. Using this setting, the expression (3.4) for $\mathcal{A}y$ becomes

$$\mathcal{A}y = \sum_{j=-\infty}^{j_{max}+1} \sum_{k \in \mathbb{Z}} \sum_{l=1}^{\infty} \frac{1}{\alpha_j} \langle y, f_{j, k, l} \rangle_{L_2(\Omega_S)} \tilde{e}_{j, k, l}, \quad (3.10)$$

where

$$\alpha_j = \begin{cases} (1 + 2^{-j_{max}})^{-1/2}, & j = j_{max} + 1, \\ (1 + 2^{-j})^{-1/2}, & j \leq j_{max}, \end{cases}$$

and

$$f_{j, k, l}(s, \theta) = \begin{cases} \psi_{j_{max}, k}^1(s) \exp(il\theta) / \sqrt{2\pi}, & j = j_{max} + 1. \\ \psi_{j, k}^2(s) \exp(il\theta) / \sqrt{2\pi}, & j \leq j_{max}. \end{cases}$$

For computation, we replaced the infinite sums in (3.10) by

$$\mathcal{A}y \approx \sum_{j=j_{min}}^{j_{max}+1} \sum_{k \in K(j)} \sum_{l=1}^L \frac{1}{\alpha_j} \langle y, f_{j, k, l} \rangle_{L_2(\Omega_S)} \tilde{e}_{j, k, l} \quad (3.11)$$

where $K(j) := \{k \in \mathbb{Z} : \text{supp}(\psi_{j, k}^1) \cap [-1, 1]\}$ for $j \leq j_{max}$, $K(j_{max} + 1) := K(j_{max})$. We used $j_{min} = 0$, $j_{max} = 3$, and $L = N_\theta$. Analogously, for the approximate solutions

z_α^δ we use

$$z_\alpha^\delta \approx \sum_{j=j_{\min}}^{j_{\max}+1} \sum_{k \in K(j)} \sum_{l=1}^L \alpha_j g_\alpha(\alpha_j^2) \langle y, f_{j,k,l} \rangle_{L_2(\Omega_S)} \tilde{e}_{j,k,l}, \quad (3.12)$$

where for the function g_α we use the filter functions of Tikhonov regularization, Landweber iteration, and the truncated SVD as defined in (1.10), respectively.

Remark 3.1. Note that since due to (1.12) for all $x \in L_2(\Omega_D)$ there holds

$$\alpha_j \langle x, e_{j,k,l} \rangle_{L_2(\Omega_D)} = \langle Ax, f_{j,k,l} \rangle_{L_2(\Omega_S)},$$

in the the computation of the dual frame functions $\tilde{e}_{j,k,l}$ the computation of the inner products $\langle x, e_{j,k,l} \rangle_{L_2(\Omega_D)}$ can be replaced by the computation of the inner products $\langle Ax, f_{j,k,l} \rangle_{L_2(\Omega_S)}$. This is advantageous, since the support of $f_{j,k,l}$ is known explicitly (cf. Figure 3.2) and thus the integration domain can be restricted.

3.2.4 Implementation of the Exponential-based Frame Decomposition

For the setup as in Theorem 3.2 we replace the infinite sum in (3.6) by

$$Ay \approx \sum_{j=j_{\min}}^{j_{\max}} \sum_{k=1}^{N_\theta} \frac{1}{\alpha_j} \langle y, w_{j,k} \rangle_{L_2(\Omega_S)} \tilde{v}_{j,k}, \quad (3.13)$$

using $j_{\min} = -\lfloor p/2 \rfloor = -30$, $j_{\max} = \lceil p/2 \rceil - 1 = 29$, and $\alpha_j = (1 + |j|^2)^{-1/4}$, which follows from our choice of $\beta = 0$. Analogously, for the approximate solutions z_α^δ we use

$$z_\alpha^\delta \approx \sum_{j=j_{\min}}^{j_{\max}} \sum_{k=1}^{N_\theta} \alpha_j g_\alpha(\alpha_j^2) \langle y, w_{j,k} \rangle_{L_2(\Omega_S)} \tilde{v}_{j,k}, \quad (3.14)$$

with the filter functions of Tikhonov regularization and Landweber iteration as above.

3.3 Numerical Results

In the following, we present some numerical results for the FDs of the Radon transform discussed above. The numerical experiments involve two regularization methods combined with an a-priori and an a-posteriori parameter choice rule for different noise levels. We also present equivalent results based on the SVD of the Radon transform, in order to compare the performance and behaviour of these methods. Note that since the SVD is a special case of the FD, the parameter choice rules discussed in Section 2 can be used for both. The truncation value for the indices in the SVD-implementation was chosen such that the number of singular functions coincides with the number of frame functions in the exponential-based setup.

For our numerical experiments we use the Shepp-Logan phantom x_{SL} depicted in Figure 3.1 (left) as the exact solution, i.e., $x^\dagger := x_{SL}$. For measuring the quality of the

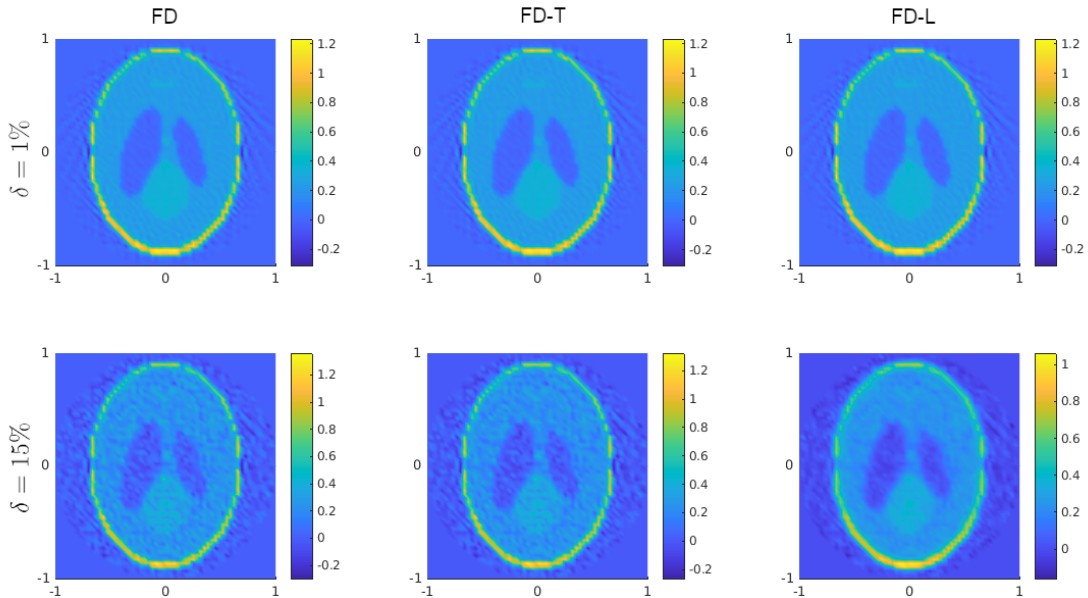


Figure 3.3: Reconstruction of the Shepp-Logan phantom using the SVD for the Radon transform using an a-priori parameter choice rule for different noise levels.

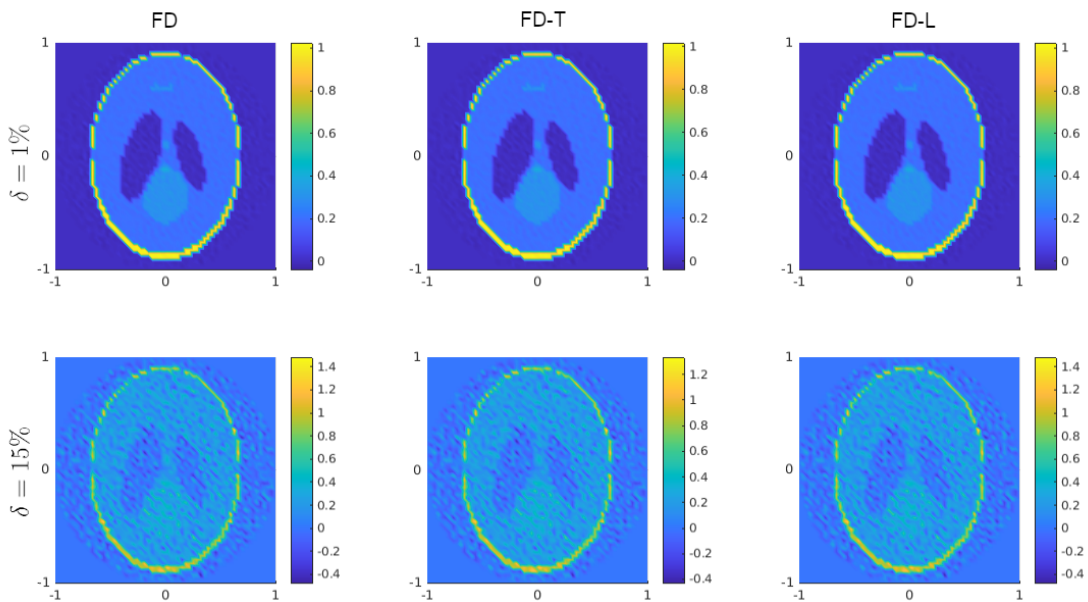


Figure 3.4: Reconstruction of the Shepp-Logan phantom using the FD for the Radon transform based on wavelet frames (3.12) using an a-priori parameter choice rule.

obtained reconstructions, we use both the relative L_2 -error $\|z_\alpha^\delta - x_{SL}\| / \|x_{SL}\|$ and the structural similarity index measure (SSIM), which is defined in [23]. The SSIM is a value in $[0, 1]$, with higher values indicating a stronger structural similarity.

Figure 3.3, 3.4, and 3.5 depict several reconstruction results using the a-priori pa-

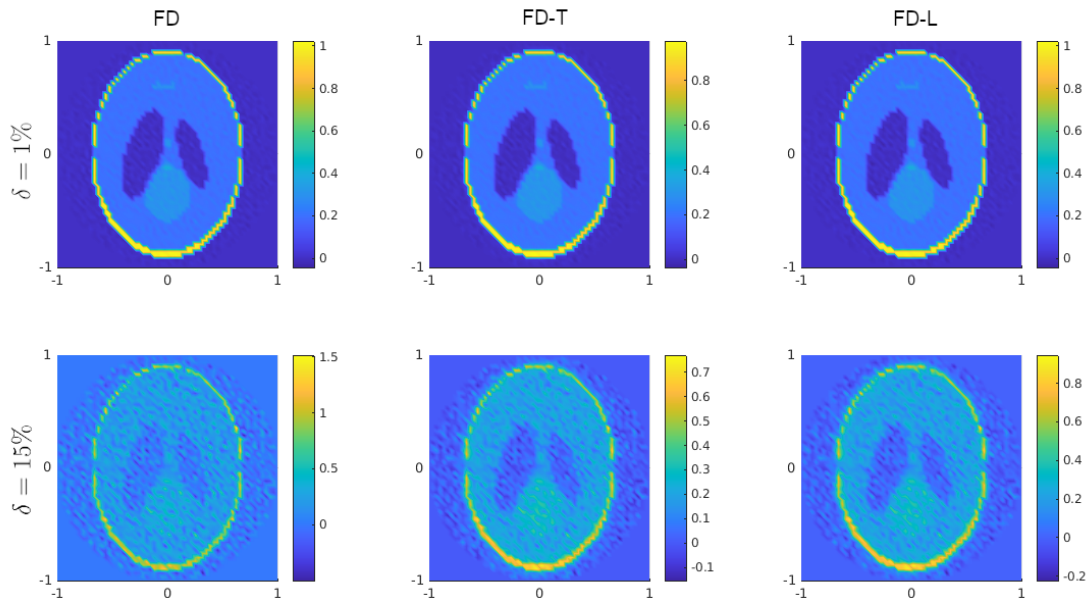


Figure 3.5: Reconstruction of the Shepp-Logan phantom using the FD for the Radon transform based on exponential frames (3.14) using an a-priori parameter choice rule.

parameter choice rule $\alpha = 0.5\delta$. The results presented in these figures are structured as follows: First column: FD without additional regularization (FD), second column: FD with Tikhonov regularization (FD-T), third column: FD with Landweber iteration (FD-L). Top row: 1% relative noise, bottom row: 15% relative noise. The corresponding error measures are collected in Table 3.1, which also includes results for our a-posteriori parameter choice rule (2.29). However, since these results are visually very similar to those obtained with the a-priori parameter choice rule, we decided not to include them in this paper. Note that since in our experiments the frame functions f_k are orthonormal, there holds $C_2 = 1$, and thus (2.28) provides a computable lower bound for τ in our a-priori parameter choice rule (2.29). However, we empirically found the choice $\tau = 0.1$ for the SVD case and $\tau = 20$ for the FD cases to lead to much better results, and thus used them in all of the presented numerical experiments.

Comparing the obtained results as summarized in Table 3.1, we see that for a relative noise level of 1%, additional regularization beyond the truncation inherent in the discretization is only beneficial for the SVD case. However, for a noise level of 15% noise, additional regularization via the Tikhonov and Landweber filter functions is often beneficial, which can be seen from the error measures, in particular from the SSIM. It appears that the additional regularization has the most impact on the SVD, while having less impact on the exponential- and the wavelet-based FDs. This can be explained by the fact that for the chosen range of the indices j we have $\alpha_j \in [0.71, 0.94]$ for the wavelet-based FD and $\alpha_j \in [0.15, 1]$ for the exponential-based FD. In contrast, the singular values σ_m of the SVD lie within the interval $[0.27, 3.54]$ in our chosen range of indices m . However, note that since these index ranges were chosen such that in both the SVD and the exponential-based FD case the same number of singular/frame

stopping rule:		a-priori			a-posteriori	
Filter function:		none	Tikh.	Landw.	Tikh.	Landw.
		Relative L_2 -error				
SVD	1% Noise	18.53%	18.53%	18.54%	18.53%	18.56%
	15% Noise	20.91%	20.75%	27.92%	20.81%	21.30%
Wav	1% Noise	2.42%	2.51%	2.42%	2.45%	2.56%
	15% Noise	25.43%	23.00%	25.43%	24.56%	24.41%
Exp	1% Noise	2.54%	5.18%	2.54%	2.72%	2.88%
	15% Noise	27.39%	27.82%	24.11%	23.69%	23.10%
		SSIM				
SVD	1% Noise	0.84	0.84	0.84	0.84	0.84
	15% Noise	0.61	0.62	0.68	0.63	0.64
Wav	1% Noise	0.98	0.98	0.98	0.98	0.98
	15% Noise	0.49	0.50	0.49	0.49	0.49
Exp	1% Noise	0.97	0.97	0.97	0.97	0.97
	15% Noise	0.48	0.57	0.59	0.51	0.51

Table 3.1: Error values for the numerical experiments with the Shepp-Logan phantom.

functions are used, we find that the FDs lead to more accurate reconstructions in the case of low noise levels than those obtained via the SVD, while the SVD shows better stability and regularization properties in the case of high noise levels, at a comparable computational cost.

Finally, Figure 3.6 illustrates the dependence of the error-measures on the regularization parameter. The marks indicate the parameters selected by the a-priori and a-posteriori parameter choice rules. In particular, note that the optimal (maximal) value of the SSIM is reached at a larger value of α than the optimal (minimal) L_2 -error.

4 Conclusion

In this paper, we considered general continuous regularization methods based on FDs for linear ill-posed problems in Hilbert spaces. In particular, we proved convergence and convergence rates results under a-priori and a-posteriori parameter choice rules analogous to those for SVD-based regularization methods. Furthermore, we applied our results to a standard tomography problem based on the Radon transform, using specific FDs based on wavelets and exponential functions. The obtained results demonstrate that FDs are a viable approach for efficiently solving linear ill-posed problems.

5 Support

SH and RR were funded by the Austrian Science Fund (FWF): F6805-N36. LW was supported by the strategic program “Innovatives OÖ 2010 plus” by the Upper Austrian

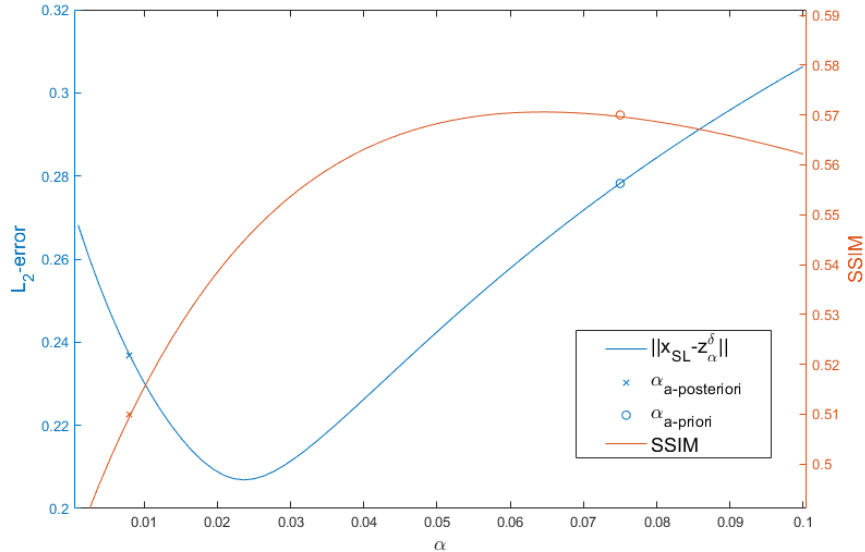


Figure 3.6: Error-plot for the exponential-based FD (3.14) with Tikhonov filter reconstructing the Shepp-Logan phantom with 15% noise. The marks show the different parameter choices. The minimal possible error is obtained at $\alpha = 0.023$ and yields an error of 20.69%. The maximal SSIM of 0.57 is obtained at $\alpha = 0.061$

Government and by the Austrian Science Fund (FWF): W1214-N15, project DK8

References

- [1] F. Abramovich and B. W. Silverman. Wavelet Decomposition Approaches to Statistical Inverse Problems. *Biometrika*, 85(1):115–129, 1998.
- [2] E. J. Candes and D. L. Donoho. Recovering edges in ill-posed inverse problems: optimality of curvelet frames. *Ann. Statist.*, 30(3):784–842, 2002.
- [3] O. Christensen. *An Introduction to Frames and Riesz Bases*. Applied and Numerical Harmonic Analysis. Springer International Publishing, 2016.
- [4] F. Colonna, G. Easley, K. Guo, and D. Labate. Radon transform inversion using the shearlet representation. *Applied and Computational Harmonic Analysis*, 29(2):232–250, 2010.
- [5] I. Daubechies. *Ten Lectures on Wavelets*. Society for Industrial and Applied Mathematics, Philadelphia, PA, 1992.
- [6] V. Dicken and P. Maass. Wavelet-Galerkin methods for ill-posed problems. *J. Inverse Ill-Posed Probl.*, 4(3):203–221, 1996.
- [7] D. L. Donoho. Nonlinear Solution of Linear Inverse Problems by Wavelet–Vaguelette Decomposition. *Applied and Computational Harmonic Analysis*, 2(2):101–126, 1995.
- [8] A. Ebner, J. Frikel, D. Lorenz, J. Schwab, and M. Haltmeier. Regularization of inverse problems by filtered diagonal frame decomposition. *ArXiv preprint*, August 2020.
- [9] H. W. Engl. *Integralgleichungen*. Wien: Springer, 1997.

- [10] H. W. Engl, M. Hanke, and A. Neubauer. *Regularization of inverse problems*. Dordrecht: Kluwer Academic Publishers, 1996.
- [11] J. Friel. Sparse regularization in limited angle tomography. *Applied and Computational Harmonic Analysis*, 34(1):117–141, 2013.
- [12] J. Friel and M. Haltmeier. Efficient regularization with wavelet sparsity constraints in photoacoustic tomography. *Inverse Problems*, 34(2):024006, 2018.
- [13] J. Friel and M. Haltmeier. Sparse Regularization of Inverse Problems by Operator-Adapted Frame Thresholding. In W. Dörfler, M. Hochbruck, D. Hundertmark, W. Reichel, A. Rieder, R. Schnaubelt, and B. Schörkhuber, editors, *Mathematics of Wave Phenomena*, pages 163–178, Cham, 2020. Springer International Publishing.
- [14] P. C. Hansen and J. S. Jørgensen. AIR Tools II: algebraic iterative reconstruction methods, improved implementation. *Numerical Algorithms*, 79(1):107–137, 2018.
- [15] S. Hubmer and R. Ramlau. A frame decomposition of the atmospheric tomography operator. *Inverse Problems*, 36(9):094001, 2020.
- [16] S. Hubmer and R. Ramlau. Frame Decompositions of Bounded Linear Operators in Hilbert Spaces with Applications in Tomography. *Inverse Problems*, 37(5):055001, 2021.
- [17] Johann Radon Institute. High Performance Computing. <https://www.ricam.oeaw.ac.at/hpc/>, 2008. [Online; accessed 21-June-2021].
- [18] A. A. Kudryavtsev and O. V. Shestakov. Estimation of the Loss Function When Using Wavelet-Vaguelette Decomposition for Solving Ill-Posed Problems. *Journal of Mathematical Sciences*, 237:804–809, 2019.
- [19] N. Lee. *Wavelet-vaguelette decompositions and homogeneous equations*. ProQuest LLC, Ann Arbor, MI, 1997. Thesis (Ph.D.)—Purdue University.
- [20] A. K. Louis. *Inverse und schlecht gestellte Probleme*. Teubner Studienbücher Mathematik. Vieweg+Teubner Verlag, 1989.
- [21] F. Natterer. *The Mathematics of Computerized Tomography*. Society for Industrial and Applied Mathematics, Philadelphia, PA, 2001.
- [22] R. Ramlau, C. Koutschan, and B. Hofmann. On the Singular Value Decomposition of n-Fold Integration Operators. In J. Cheng, S. Lu, , and M. Yamamoto, editors, *Inverse Problems and Related Topics*, pages 237–256. Springer Singapore, 2020.
- [23] Z. Wang, A.C. Bovik, H. R. Sheikh, and E. P. Simoncelli. Image quality assessment: from error visibility to structural similarity. *IEEE Transactions on Image Processing*, 13(4):600–612, 2004.
- [24] L. Weissinger. Realization of the Frame Decomposition of the Atmospheric Tomography Operator. Master’s thesis, JKU Linz, 2020.